Quad-Rotor Unmanned Aerial Vehicle Helicopter Modelling & Control

Regular Paper

Yogianandh Naidoo[1,*], Riaan Stopforth[2] and Glen Bright[3]

1 School of Mechanical Engineering, University of KwaZulu Natal
2 Mechatronics and Robotics Research Group (MR₂G) Search and Rescue Division, University of KwaZulu-Natal
3 Mechatronics and Robotics Research Group (MR₂G), University of KwaZulu-Natal

*Corresponding Author Email: 205506529@ukzn.ac.za

Abstract This paper presents the investigation of the modelling and control of a quad-rotor helicopter and forms part of research involving the development of an unmanned aerial vehicle (UAV) to be used in search and rescue applications. Quad-rotor helicopters consist of two pairs of counter rotating rotors situated at the ends of a cross, symmetric about the centre of gravity, which coincides with the origin of the reference system used. These rotors provide the predominant aerodynamic forces which act on the rotorcraft, and are modelled using momentum theory as well as blade element theory. From this, one can determine the expected payload capacity and lift performance of the rotorcraft. The Euler-Lagrange method has been used to derive the defining equations of motion of the six degree-of-freedom system. The Lagrangian was obtained by modelling the kinetic and potential energy of the system and the external forces obtained from the aerodynamic analysis. Based on this model, a control strategy was developed using linear PD controllers. A numerical simulation was then conducted using MATLAB® Simulink®. First, the derived model was simulated to investigate the behaviour of the rotorcraft, and then a second investigation was conducted to determine the effectiveness of the implemented control system. The results and findings of these investigations are then presented and discussed.

1. Introduction

1.1 Background

The following dynamics model pertains to a quad-rotor unmanned aerial vehicle (UAV) helicopter which is intended to be used as a search and rescue field robot. The use of a rotorcraft allows for high degrees of manoeuvrability, including the ability to hover. The ultimate aim is to develop a self-stabilizing and self-navigating UAV capable of performing autonomous take-offs and landings similar to the unmanned aerial system (UAS) developed at Stellenbosch University (IK Peddle, 2009). This way, the UAV is able to transmit data to operators situated at a safe vantage point at the scene of a disaster. In most cases, the state of such disaster sites is too dangerous for human expedition. By using robots, the site can be properly analysed and better decisions can be made with regards to the execution of a rescue operation (D Greer, 2002). The use of a hovering robot as a search and rescue robot means that rescue team response times can be kept to a minimum. This is important as it is crucial to seek victims as soon as possible to ensure the

best possible survival rate. One of the most successful multi-rotor platforms is the Draganflyer X-Pro (Sikiric, 2008). This was used as a platform for research conducted at the Royal Institute of Technology in Stockholm, Sweden. The reason for pursuing a multi-rotor rotorcraft is due to the small rotor spans allowable, thus minimising the damage in the event of a collision. The large rotor spans of conventional helicopters are too dangerous to manoeuvre in confined spaces as well as near injured victims.

It must be noted that this is not the only method for deriving a mathematical model for a system such as this, but is the preferred method for the author. Research conducted at the University of South Florida (N Aldawoodi, 2004) presented a heuristic technique that applies simulated annealing search to derive mathematical equations.

1.2 Quad-rotor Helicopter Structure

The structure of a quad-rotor helicopter is a simple one, basically comprising of four rotors attached at the ends of a symmetric cross. A proposed structure is presented in figure 1.

The key features that should be taken into account in such a structure are symmetry and rigidity. To avoid unstable flight, the structure should be as rigid as possible, while maintaining the lightest possible weight. The best way to achieve this is through lightweight alloys or composites. Symmetry is also of great importance for stability. The centre of gravity (COG) should be kept as close to the middle of the rotorcraft as possible, as depicted in figure 3.

Figure 1. Proposed quad-rotor helicopter structure

1.3 System Integration

The electronic system integration is presented in figure 2. The key components are a microcontroller, electronic speed controllers (ESC's), an attitude and heading reference system (AHRS), a communication interface between the UAV and the user, a vision system and suitable power distribution.

The microcontroller receives data from the AHRS, vision system and communication interface, which is then processed so that orders can be executed to the ESC's to control the motor.

The AHRS measures the inertial movements of the UAV. It comprises of an inertial measurement unit (IMU) and a global positioning system (GPS). The IMU contains 3-axis accelerometers and gyroscopes to measure translational and rotational body motion respectively. It also consists of a magnetometer, which acts as a digital compass and determines the heading of the UAV. The GPS is used to determine the location of the rotorcraft. Another component which could be added to the AHRS is a pressure sensor to measure altitude. However, these sensors are only suitable for high altitude applications and therefore, it would be more appropriate to use rangefinder to determine the altitude of the UAV. These rangefinders could be either sonar or laser and form as part of the vision system. The vision system is used to detect possible obstacles in the path of the rotorcraft, as well as transfer visual data to the user via the communication interface.

Lithium Polymer (LiPo) batteries are the most suitable power source in such applications due to their lightweight properties. Power is distributed to all the electronics in the system via a power distribution board (PDB).

1.4 Flight Dynamics

Like a conventional helicopter, a quad-rotor helicopter is a six-degree-of-freedom, highly non-linear, multivariable, strongly coupled, and under-actuated system. The main forces and moments acting on a quad-rotor helicopter are produced by its rotors (W Daobo, 2008). It is arguably a simpler setup from its dual rotor counterpart, as quad-rotor helicopters can be controlled exclusively by variation in motor speed. Two pairs of rotors rotate in opposite directions to balance the total torque of the system. Figure 3 (W Daobo, 2008), shows a free body diagram of a typical quad-rotor type helicopter. As shown, only two reference frames are used (the earth fixed frame, E, and the body frame, B), unlike that of a conventional helicopter which has three. The reason for this is that the rotors of a quad-rotor helicopter are fixed;

whereas the main rotor of a conventional helicopter has actuators to control the roll and pitch angles, which moves independent of the fuselage.
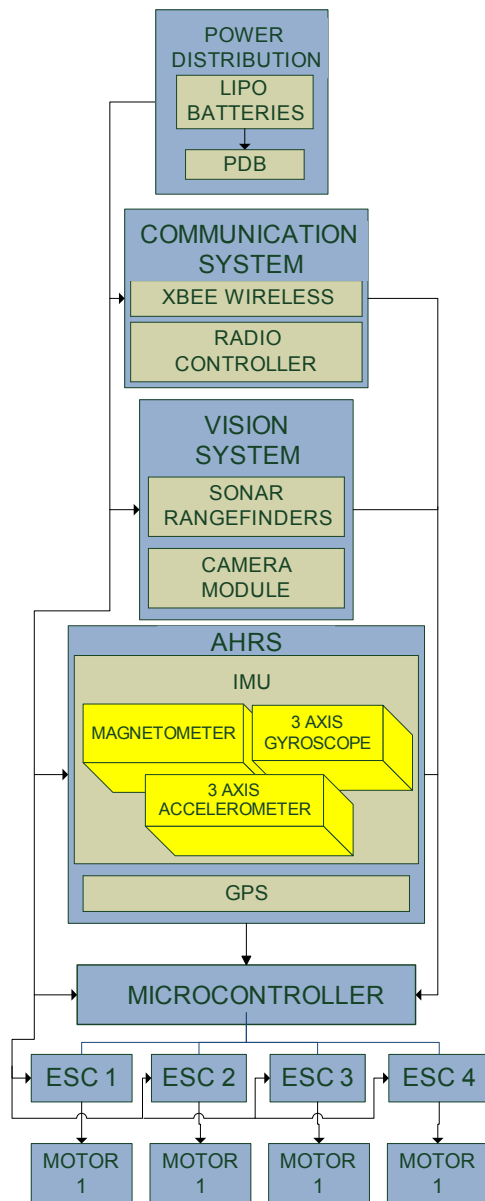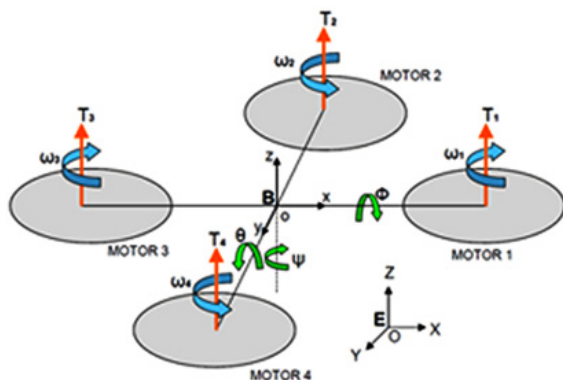

Figure 2. Electronic system integration

Figure 3. Free body diagram of a quad-rotor helicopter

A quad-rotor setup is controlled by manipulating thrust forces from individual rotors as well as balancing drag torque. For hovering, all rotors apply a constant thrust force as illustrated in figure 4(c), thus keeping the aircraft balanced. To control vertical movement, the motor speed is simultaneously increased or decreased, thus having a lower or higher total thrust but still maintaining balance. For attitude control, the yaw angle (ψ) may be controlled by manipulating the torque balance, depending on which direction the aircraft should rotate. The total thrust force still remains balanced, and therefore no altitude change occurs. This can be shown in figures 4(a) and 4(b). In a similar way, the roll angle (ϕ) and pitch angle (θ) can be manipulated applying differential thrust forces on opposite rotors, as illustrated in figure 4(d) (Stepaniak, 2008; J Kim, 2010).

Although this may seem simple in theory, practically, there will be many factors which need to be taken into account. One of the greatest challenges will be to achieve stability in an outdoor environment. Especially a disaster area where there will be many obstacles and possibly harsh winds.

1.5 Rotor Aerodynamics

As with conventional helicopters, most of the aerodynamic significance of quad-rotor helicopters lies within their rotors. The propellers, motors and batteries determine the payload and flight time performance of the aircraft. The rotors, especially, influence the natural dynamics and power efficiency. Research at the Australian National University (P Pounds, 2004) has shown that an approximate understanding of helicopter rotor performance can be obtained from the momentum theory of rotors. This performance is very important. As a
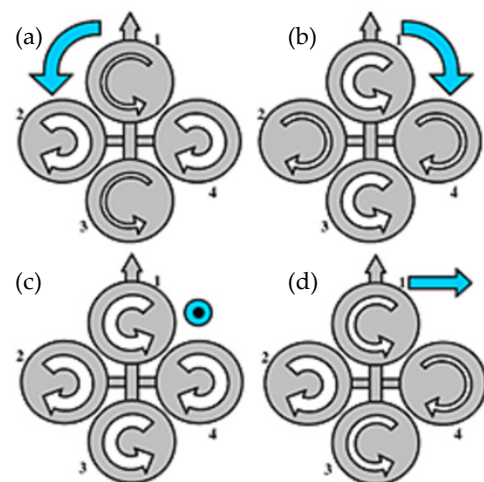

Figure 4. Quad-rotor dynamics, (a) and (b) difference in torque to manipulate the yaw angle (ψ); (c) hovering motion and vertical propulsion due to balanced torques; and (d) difference in thrust to manipulate the pitch angle (θ) the roll angle (ϕ).

www.intechweb.org
www.intechopen.com

Yogianandh Naidoo, Riaan Stopforth and Glen Bright: 141
Quad-Rotor Unmanned Aerial Vehicle Helicopter Modelling & Control

search and rescue robot, the rotorcraft will be exposed to harsh environments where it should be able to produce enough thrust force to counter any bursts of external forces applied to it in order for it to stabilise itself. Further, it should be able to carry the payload of equipment such as cameras, sensors, etc.

2. Rotor Aerodynamics: Momentum Theory and Blade Element Theory

Momentum theory can be used to provide relationships between thrust, induced velocity and power in the rotor. Using energy conservation (P Pounds, 2004), it can be shown that in hover,

$$T = 2\rho A v_i^2 \qquad (1)$$

Where T is the thrust, ρ is the density of air, A is the area of the rotor, and v_i is the induced air velocity at the rotor. Blade element theory (P Pounds, 2004; JF Douglas, 2005) is particularly useful for airfoil and rotor performance. The forces and moment developed on a uniform wing are modelled by,

$$L = C_L \frac{1}{2}\rho v^2 c \qquad (2)$$

$$D = C_D \frac{1}{2}\rho v^2 c \qquad (3)$$

$$M = C_M \frac{1}{2}\rho v^2 c^2 \qquad (4)$$

Where, for unit span, L is the lift produced, D is the profile drag and M is the pitching moment. v is the velocity of the wing through the air and c is the chord length. C_L, C_D and C_M are dimensionless coefficients of lift, drag and moment, respectively. They are dependent upon the wing's Reynolds Number (RE), Mach number and angle of attack (α). For a rotor with angular velocity ω, the linear velocity at each point along the rotor is proportional to the radial distance from the rotor shaft,

$$v = \omega R \qquad (5)$$

By integrating lift and drag along the length of the blade, equivalent rules may be produced for the entire rotor (P Pounds, 2004).

$$F_i = b\omega_i^2 \qquad (6)$$

$$\tau_i = d\omega_i^2 \qquad (7)$$

Where b and d are the thrust and drag moment constants respectively.

$$b = C_T \rho A R^2 \qquad (8)$$

$$d = C_Q \rho A R^3 \qquad (9)$$

F_i is the thrust produced by rotor i, τ_i is the drag moment and R is the rotor radius. C_T and C_Q are dimensionless thrust and drag moment coefficients. It is also evident from equation (6) and equation (7) that the thrust force and rotor torque is directly proportional to the angular velocity of the rotor. This is a useful relationship, as the rotor angular velocity can be controlled by the motor, thus, the thrust force and drag moment can also be controlled by the motor. Smaller rotors require higher speeds and more power than larger rotors for the same thrust (P Pounds, 2004). The respective total thrust force and rotor torque of the system is,

$$f = \sum_{i=1}^{4} F_i \qquad (10)$$

Besides the thrust force and the drag moment, which are the predominant aerodynamic forces and moments created by a rotor, there exist three other external aerodynamic influences (R Siegwart, 2007) which act on a propeller. These may be illustrated in figure 5. The first is called ground effect. This refers to the variation of the thrust co-efficient when the rotor is in close proximity to the ground. The ground effect thrust force may be described as,

$$F_{IGE} = C_T^{IGE} \rho A (\omega_i R)^2 \qquad (11)$$

Where, C_T^{IGE} is the thrust co-efficient near ground level. Another influential aerodynamic force occurs as a result of horizontal forces acting on all the blade elements, known as the hub force,

$$H = C_H \rho A (\omega_i R)^2 \qquad (12)$$

C_H is the hub force co-efficient.

The third influence, referred to as rolling moment R_m, is the combined moment due to the lift at each point along the radius of the rotor,

$$R_m = C_{R_m} \rho A (\omega_i R)^2 R \qquad (13)$$
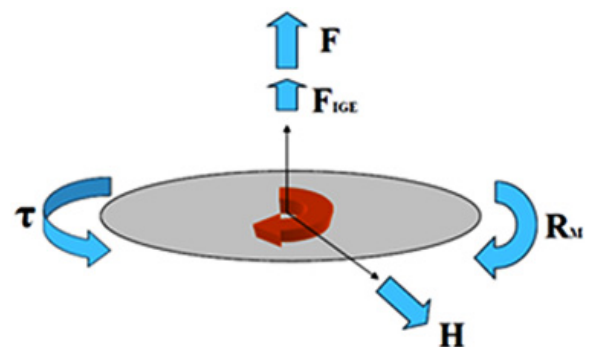
Where, C_{R_m} is the rolling moment co-efficient.

Figure 5. Aerodynamic forces and moments on a rotor

3. Co-ordinate Reference Frames and the Rotation Matrix

There are two co-ordinate reference frames when analysing quad-rotor helicopter dynamics. The first is the earth fixed frame, labelled E in figure 3. The other is the body reference frame, labelled B, which is a rotating co-ordinate frame with the origin, situated at the centre of gravity of the rotorcraft. All rotation occurs about the origin, and can be described by specifying an axis of rotation as well as an angle by which the frame is being rotated. This type of rotation is described in Euler's Theorem (A Tewari, 2007), which states that the relative orientation of any pair of co-ordinate frames is uniquely determined by a rotation by angle, Φ, about a fixed axis through the common origin, called the Euler axis. This unique rotation is termed the principal angle. A graphical representation can be shown in figure 6, where the vector e is the Euler axis and the rotation angle Φ represents the principal angle.

Since the body motion sensors will be attached directly to the reference frame, the readings will be with relation to the rotated frame. Therefore, it is important to obtain these co-ordinates in order to successfully model the system. This is done through a rotation matrix (A Tewari, 2007; P Castillo R. a., 2005). If unit vectors, *i; j* and *k*, in the direction of the *x; y* and *z* axes respectively, are rotated to the orientation of *x'; y'* and *z'*, with unit vectors *i', j'* and *k'* respectively, then these new unit vectors can be represented in terms of the original orientation with the use of a rotation matrix (A Tewari, 2007),

$$\begin{bmatrix} i' \\ j' \\ k' \end{bmatrix} = R \begin{bmatrix} i \\ j \\ k \end{bmatrix} \tag{14}$$

Where,

$$R = \begin{bmatrix} i' \cdot i & i' \cdot j & i' \cdot k \\ j' \cdot i & j' \cdot j & j' \cdot k \\ k' \cdot i & k' \cdot j & k' \cdot k \end{bmatrix} \tag{15}$$
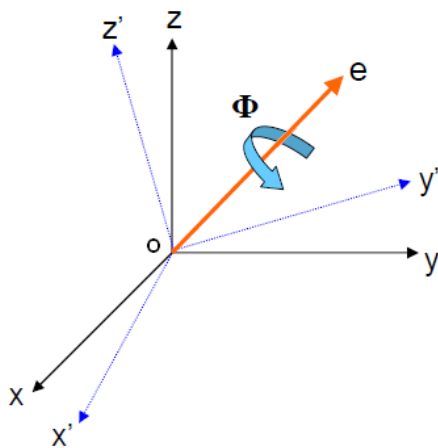
Figure 6. Euler axis and principal angle on a rotating co-ordinate frame

The rotation matrix R is orthogonal, which implies that the matrix transposed would be equivalent its inverse form. For every rotation, a rotation matrix exists. If the co-ordinate frame had to go through a second rotation, R', then the resultant rotation from its original orientation would be R'', where,

$$R'' = R \cdot R' \tag{16}$$

This is an extremely useful characteristic, as a full rotation of a system can be described as a product of the rotations about its *x*, *y* and *z* axes,

$$R = R_x \cdot R_y \cdot R_z \tag{17}$$

Where for a roll angle ϕ about the x-axis, pitch angle θ about the y-axis and yaw angle ψ about the z-axis (A Tewari, 2007),

$$R_x = \begin{bmatrix} 1 & 0 & 0 \\ 0 & \cos\phi & \sin\phi \\ 0 & -\sin\phi & \cos\phi \end{bmatrix} \tag{18}$$

$$R_y = \begin{bmatrix} \cos\theta & 0 & -\sin\theta \\ 0 & 1 & 0 \\ \sin\theta & 0 & \cos\theta \end{bmatrix} \tag{19}$$

$$R_z = \begin{bmatrix} \cos\psi & \sin\psi & 0 \\ -\sin\psi & \cos\psi & 0 \\ 0 & 0 & 1 \end{bmatrix} \tag{20}$$

Resulting in a rotation matrix R, where $c\theta$ represents $cos\theta$ and $s\theta$ represents $sin\theta$,

$$R = \begin{bmatrix} c\theta c\psi & c\theta s\psi & -s\theta \\ s\phi s\theta c\psi - c\phi s\psi & s\phi s\theta s\psi + c\phi c\psi & s\phi c\theta \\ c\phi s\theta c\psi + s\phi s\psi & c\phi s\theta s\psi - s\phi c\psi & c\phi c\theta \end{bmatrix} \tag{21}$$

4. Quad-Rotor Dynamics Modelling

The Euler-Lagrange method (P Castillo R. a., 2005; P Castillo A. a., 2004) is used to model the flight dynamics of the rotorcraft. The model stands under the assumptions that the motor dynamics are relatively fast and may therefore be neglected. Also, the rotor blades are assumed to be perfectly rigid and no blade flapping occurs. Although this does occur in reality, the effects of this phenomenon are minuscule and will be considered later in the research. External wind forces are also not considered at this stage. The equations of motion are developed in terms of the translational and rotational parameters of the six-degree-of-freedom system, using generalised co-ordinates in a vector q,

www.intechweb.org
www.intechopen.com

Yogianandh Naidoo, Riaan Stopforth and Glen Bright: 143
Quad-Rotor Unmanned Aerial Vehicle Helicopter Modelling & Control

$$q = \begin{bmatrix} x & y & z & \phi & \theta & \psi \end{bmatrix}^T \qquad (22)$$

These co-ordinates can be separated into translational, ξ, and rotational, η, co-ordinates where,

$$\xi = \begin{bmatrix} x & y & z \end{bmatrix}^T \text{ and } \eta = \begin{bmatrix} \phi & \theta & \psi \end{bmatrix}^T \qquad (23)$$

Therefore,

$$q = \begin{bmatrix} \xi & \eta \end{bmatrix}^T \qquad (24)$$

A Lagrangian is obtained by modelling the energy of the system, where the difference between kinetic and potential energy is taken. Kinetic energy of the system is modelled for both translational and rotational motion. The potential energy of the system is related only to the altitude of the rotorcraft. The Lagrangian, L, can be expressed as,

$$L = T - U \qquad (25)$$

Where, T is the kinetic energy and U is the potential energy of the system. The total kinetic energy of the system is the sum of the energy due to the translational motion and rotational motion. Therefore, the final expression obtained for the Lagrangian is,

$$L(q,\dot{q}) = \frac{1}{2}\dot{\xi}^T m \dot{\xi} + \frac{1}{2}\dot{\eta}^T I \dot{\eta} - mgz \qquad (26)$$

This can be reduced to,

$$L(q,\dot{q}) = \frac{1}{2}m\left(\dot{x}^2 + \dot{y}^2 + \dot{z}^2\right)$$
$$+ \frac{1}{2}\left(I_{xx}\dot{\phi}^2 + I_{yy}\dot{\theta}^2 + I_{zz}\dot{\psi}^2\right) - mgz \qquad (27)$$

For this analysis, the Euler-Lagrange equation with an external generalised force (P Castillo R. a., 2005) is used.

$$\frac{d}{dt}\frac{\partial L}{\partial \dot{q}} - \frac{\partial L}{\partial q} = F \qquad (28)$$

Where, the force F represents all the external forces acting on the body of the rotorcraft. Again, this can be split into translational, F_ξ and rotational, τ components. Where,

$$F_\xi = \begin{bmatrix} F_x & F_y & F_z \end{bmatrix}^T \qquad (29)$$

And,

$$\tau = \begin{bmatrix} \tau_\phi & \tau_\theta & \tau_\psi \end{bmatrix}^T \qquad (30)$$

Therefore,

$$F = \begin{bmatrix} F_\xi & \tau \end{bmatrix}^T \qquad (31)$$

The PDE's $\dfrac{d}{dt}\dfrac{\partial L}{\partial \dot{q}}$ and $\dfrac{\partial L}{\partial q}$ can be expressed as,

$$\frac{d}{dt}\frac{\partial L}{\partial \dot{q}} = \begin{bmatrix} m\ddot{x} \\ m\ddot{y} \\ m\ddot{z} \\ I_{xx}\ddot{\phi} + \dot{I}_{xx}\dot{\phi} \\ I_{yy}\ddot{\theta} + \dot{I}_{yy}\dot{\theta} \\ I_{zz}\ddot{\psi} + \dot{I}_{zz}\dot{\psi} \end{bmatrix} \qquad (32)$$

And,

$$\frac{\partial L}{\partial q} = \begin{bmatrix} 0 & 0 & -mg & 0 & 0 & 0 \end{bmatrix}^T \qquad (33)$$

The only forces acting on the body are those from the rotor. The translational forces are the thrust forces resulting from each rotor, and the rotational forces are due to the drag moment as well as the moment caused by thrust forces from opposite rotors about the centre of gravity. It must be noted that hub force, ground effect and gyro effects were not taken into account, as the model was developed for the purpose of designing a control system around it, and thus should be kept as simple as possible, with only the main effects being taken into account. Therefore the translational force is,

$$F_{rotor} = \begin{bmatrix} 0 & 0 & f \end{bmatrix}^T \qquad (34)$$

Where, f is the total thrust force. However, this force is always in the z-direction of the body reference frame. In order to obtain a force that will correlate with the global co-ordinates and sensor readings, the rotation matrix discussed in equation (21) is used. This allows the author to compare sensor readings with calculated values to find a correlation between theoretical and measured parameters. Therefore,

$$F_\xi = R.F_{rotor} \qquad (35)$$

It can be seen that,

$$F_\xi = \begin{bmatrix} -f\sin\theta \\ f\sin\phi\cos\theta \\ f\cos\phi\cos\theta \end{bmatrix} \qquad (36)$$

For the rotational component τ, moments are taken from about the centre of gravity in the roll and pitch directions. Therefore,

$$\tau_\phi = (F_{M3} - F_{M1})l \qquad (37)$$

$$\tau_\theta = (F_{M2} - F_{M4})l \qquad 38)$$

Where, l is the linear distance from the centre of the rotor to the centre of gravity. In the direction of yaw, the sum of all the drag moments produced by the rotors are taken into account,

$$\tau_\psi = \sum_{i=1}^{4} \tau_{Mi} \qquad (39)$$

Where, τ_{Mi} is the torque produced by rotor i. Therefore, the total force function can be represented as the following vector,

$$F = \begin{bmatrix} -f\sin\theta \\ f\sin\phi\cos\theta \\ f\cos\phi\cos\theta \\ (F_{M3} - F_{M1})l \\ (F_{M2} - F_{M4})l \\ \sum_{i=1}^{4} \tau_{Mi} \end{bmatrix} \qquad (40)$$

Thus, the Euler-Lagrange equation, together with equations (32), (33) and (40) yields,

$$\begin{bmatrix} m\ddot{x} \\ m\ddot{y} \\ m\ddot{z} \\ I_{xx}\ddot{\phi} + \dot{I}_{xx}\dot{\phi} \\ I_{yy}\ddot{\theta} + \dot{I}_{yy}\dot{\theta} \\ I_{zz}\ddot{\psi} + \dot{I}_{zz}\dot{\psi} \end{bmatrix} + \begin{bmatrix} 0 \\ 0 \\ mg \\ 0 \\ 0 \\ 0 \end{bmatrix} = \begin{bmatrix} -f\sin\theta \\ f\sin\phi\cos\theta \\ f\cos\phi\cos\theta \\ (F_{M3} - F_{M1})l \\ (F_{M2} - F_{M4})l \\ \sum_{i=1}^{4} \tau_{Mi} \end{bmatrix} \qquad (41)$$

Therefore,

$$\ddot{q} = \begin{bmatrix} \ddot{x} \\ \ddot{y} \\ \ddot{z} \\ \ddot{\phi} \\ \ddot{\theta} \\ \ddot{\psi} \end{bmatrix} = \begin{bmatrix} -\dfrac{f}{m}\sin\theta \\ \dfrac{f}{m}\sin\phi\cos\theta \\ \dfrac{f}{m}\cos\phi\cos\theta - g \\ \dfrac{1}{I_{xx}}\left((F_{M3} - F_{M1})l - \dot{I}_{xx}\dot{\phi}\right) \\ \dfrac{1}{I_{yy}}\left((F_{M2} - F_{M4})l - \dot{I}_{yy}\dot{\theta}\right) \\ \dfrac{1}{I_{zz}}\left(\sum_{i=1}^{4} \tau_{Mi} - \dot{I}_{zz}\dot{\psi}\right) \end{bmatrix} \qquad (42)$$

Near hover, the angular rates can be taken to be negligible.

5. Quad-Rotor Control

Attitude (ϕ, θ and ψ) and altitude (z) had to be taken into account in order to stabilise the rotorcraft. Position (x and y) is dependent on the roll and pitch angle orientation. Thus, the position can be controlled via attitude control. Therefore, the system is an under actuated one, having six degrees of freedom and only four control inputs. Essentially, all manoeuvres that are executed by the rotorcraft are resultant from the manipulation of thrust and drag moment created by the four rotors. These parameters are related using the relationship described in equation (6) and equation (7). It is evident from this that by controlling the rotational speed of the motors, one can effectively control the rotorcraft. Therefore, the following are chosen for control inputs based on works conducted at Lausanne (S Bouabdallah, 2007) and Stanford University (H Huang, 2009),

$$u_1 = b\left(\omega_1^2 + \omega_2^2 + \omega_3^2 + \omega_4^2\right) \qquad (43)$$

$$u_2 = b\left(\omega_3^2 - \omega_1^2\right)l \qquad (44)$$

$$u_3 = b\left(\omega_2^2 - \omega_4^2\right)l \qquad (45)$$

$$u_4 = d\left(\omega_1^2 - \omega_2^2 + \omega_3^2 - \omega_4^2\right) \qquad (46)$$

Where, u_1, u_2, u_3 and u_4 are control inputs for altitude, roll, pitch and yaw respectively. From this, the simplified model derived in equation (42) becomes,

$$\ddot{q} = \begin{bmatrix} \ddot{x} \\ \ddot{y} \\ \ddot{z} \\ \ddot{\phi} \\ \ddot{\theta} \\ \ddot{\psi} \end{bmatrix} = \begin{bmatrix} -\dfrac{f}{m}\sin\theta \\ \dfrac{f}{m}\sin\phi\cos\theta \\ \dfrac{f}{m}\cos\phi\cos\theta - g \\ \dfrac{1}{I_{xx}}u_2 \\ \dfrac{1}{I_{yy}}u_3 \\ \dfrac{1}{I_{zz}}u_4 \end{bmatrix} \qquad (47)$$

It is evident from equation (47) that the simplified system is linear and not coupled. Thus, a linear PD controller design was chosen to be used.

The control inputs described in equation (43) to equation (46) may be represented in vector form,

$$\begin{bmatrix} u_1 \\ u_2 \\ u_3 \\ u_4 \end{bmatrix} = \begin{bmatrix} b & b & b & b \\ -bL & 0 & bL & 0 \\ 0 & bL & 0 & -bL \\ d & -d & d & -d \end{bmatrix} \begin{bmatrix} \omega_1^2 \\ \omega_2^2 \\ \omega_3^2 \\ \omega_4^2 \end{bmatrix} \quad (47)$$

Equation (47) can be rearranged to be found in terms of the rotational speed vector,

$$\begin{bmatrix} \omega_1^2 \\ \omega_2^2 \\ \omega_3^2 \\ \omega_4^2 \end{bmatrix} = \begin{bmatrix} \dfrac{1}{4b} & -\dfrac{1}{2bL} & 0 & \dfrac{1}{4d} \\ \dfrac{1}{4b} & 0 & \dfrac{1}{2bL} & -\dfrac{1}{4d} \\ \dfrac{1}{4b} & \dfrac{1}{2bL} & 0 & \dfrac{1}{4d} \\ \dfrac{1}{4b} & 0 & -\dfrac{1}{2bL} & -\dfrac{1}{4d} \end{bmatrix} \begin{bmatrix} u_1 \\ u_2 \\ u_3 \\ u_4 \end{bmatrix} \quad (48)$$

From this, the desired motor speed may be computed so that it can then be sent to the motor controllers. The columns of the matrix in equation (48) correspond to each control input, and the rows correspond to the square of the rotational speed of each motor. Thus, the square root of each row must be computed before the values can be sent to the controller. There are four feedback control loops (figure 7) which are seperate from each other, which for a PD controller, takes the form,

$U = k_P(\text{proportional error}) + k_d(\text{derivative error})$

The PD controllers for altitude, roll, pitch and yaw respectively are,

$$U_1 = k_{p_{ALT}}\left(y_{ref} - y\right) + k_{d_{ALT}}\left(\dot{y}_{ref} - \dot{y}\right) \quad (49)$$

$$U_2 = k_{p_{ROLL}}\left(\phi_{ref} - \phi\right) + k_{d_{ROLL}}\left(\dot{\phi}_{ref} - \dot{\phi}\right) \quad (50)$$

$$U_3 = k_{p_{PITCH}}\left(\theta_{ref} - \theta\right) + k_{d_{PITCH}}\left(\dot{\theta}_{ref} - \dot{\theta}\right) \quad (51)$$

$$U_4 = k_{p_{YAW}}\left(\psi_{ref} - \psi\right) + k_{d_{YAW}}\left(\dot{\psi}_{ref} - \dot{\psi}\right) \quad (52)$$

These feedback control loops will be implemented using a microcontroller as expalined in figure 2.
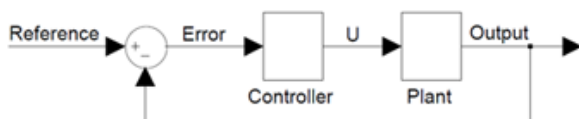

Figure 7. Feedback control loop

6. Model Simulation

The mathematical model described by equation (42) was simulated on MATLAB® Simulink®, with motor speed and basic system parameters (listed in Table 1) as inputs with the thrust, torque, q, $\dot{q}$ and $\ddot{q}$ as outputs. The thrust forces and rotor torques were modelled around equations (6) and (7).

m	kg	4
l	m	0.3
R	m	0.15
ρ	kg/m³	1.204
C_T	-	0.5
C_Q	-	0.08

Table 1. Constant model parameters

To investigate if the simulation describes the behaviour of the rotorcraft, four simulations were conducted with the motor inputs specified in Table 2. These simulations were strategically chosen to investigate lift, yawing, pitching and rolling motion respectively. First, they were conducted with no control systems implemented, and then the effects of the control system were investigated, using the same input data.

6.1 Dynamic Model Without Control

The first simulation investigated the upward lift behaviour by applying equivalent speeds of 230 rpm to each motor to create a constant total lift of 41.63 N. The resultant upward acceleration and velocity are shown in figure 8 and figure 9. This correlates to the expected upward acceleration, however, depicts an ideal situation without any external wind forces being compensated for.

Simulation Number	Motor Speed (rad/s)			
	Motor 1 (CW)	Motor 2 (CCW)	Motor 3 (CW)	Motor 4 (CCW)
1	230	230	230	230
2	231	229	231	229
3	230	229	230	231
4	229	230	231	230

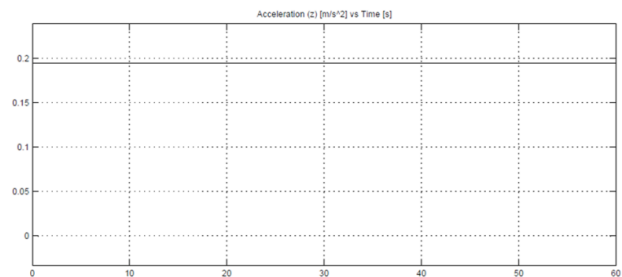**Table 2.** Simulation motor speed inputs

Figure 8. Graph of Acceleration (vertical-axis) vs Time (horizontal-axis)
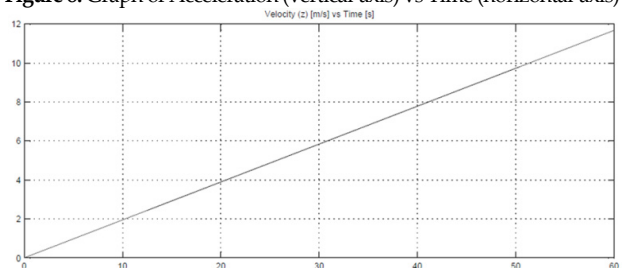

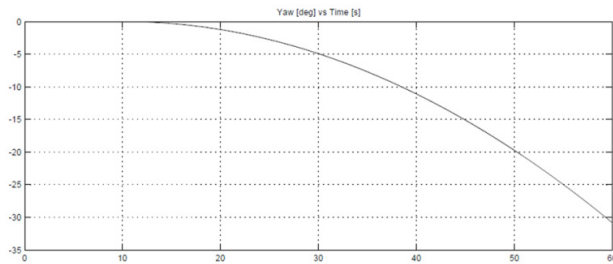**Figure 9.** Graph of Speed (vertical-axis) vs Time (horizontal-axis)

Figure 10. Graph of Yaw (vertical-axis) vs Time (horizontal-axis)
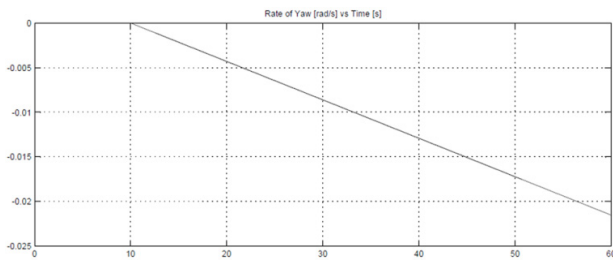

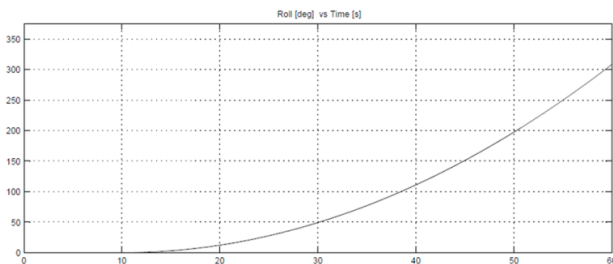**Figure 11.** Graph of Yaw Rate (vertical-axis) vs Time (horizontal-axis)

Figure 12. Graph of Roll (vertical-axis) vs Time (horizontal-axis)

The second simulation investigated the yawing motion of the rotorcraft. Here, both clockwise rotating rotors were set to rotate faster than the counter-clockwise rotating rotors, resulting in a constant counter-clockwise angular acceleration of 0.1235 rad/s². This behaviour is described in figure 10 and figure 11.

The third and fourth simulations investigate the stability of the rotorcraft with regards to rotational motion in the pitching and rolling directions. In each case, one rotor was chosen to rotate faster than motors adjacent to it, and the motor opposite to it chosen to rotate slower.

As noted in figure 12, the roll angle increases to almost an entire revolution in the one minute simulation time. This behaviour is unstable, and control is therefore required. The resultant translational motion is also unstable. An imbalance of torque was also noted.

6.2 Model Simulation With Control

After recording the behaviour of the derived mathematical model, simulations were conducted to investigate the effects of the control design on the system. The simulation inputs were identical to those in section 6.1.

6.2.1 Altitude control

The first simulation concentrated on altitude. The controller implemenred is the one described in equation (49). The aim of the simulation was to get the rotorcraft to hover at a constant altitude of 10 m. Figure 13, shows the natural response of the system without any control implemented. Figure 14 shows the effects on the system when the controller is implemented. It is clear from this comparison that the control design is effective, where a steady state is achieved.
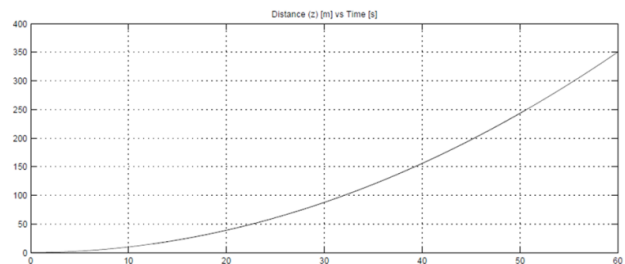

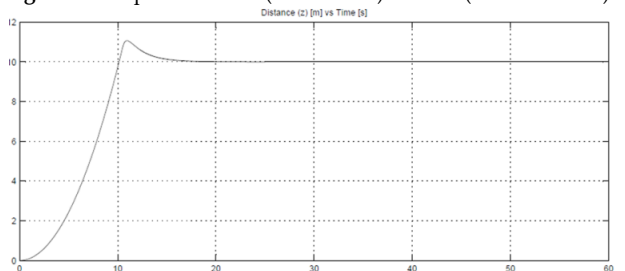**Figure 13.** Graph of Altitude (vertical axis) vs Time (horizontal axis)

Figure 14. Graph of Altitude (vertical axis) vs Time (horizontal axis)

6.2.2. Yaw Control

The yaw controller implemented during this simulation is based on equation (52). The aim of this simulation was to obtain a desired yaw angle of zero. This was effectively achieved with minimal response time, as shown in figure 15 and figure 16. This is evident if one compares the natural response, depicted in figure 10 and figure 11, to the controlled response.
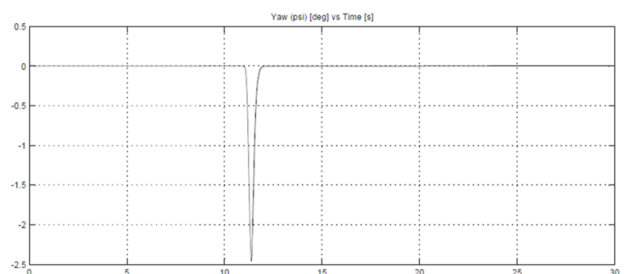

Figure 15. Graph of Yaw vs Time

6.2.3 Roll/Pitch Control

The controllers implemented for pitch and roll control can be described in equations (50) and (51) respectively.

www.intechweb.org
www.intechopen.com

Yogianandh Naidoo, Riaan Stopforth and Glen Bright:
Quad-Rotor Unmanned Aerial Vehicle Helicopter Modelling & Control   147

These parameters are extremely important to both stabilise the rotorcraft, as well as manipulate latitudinal position. However, since the aim of the simulation was to stabilise the rotorcraft while it is hovering, the desired reference values were set to zero. This was achieved to an extent. Figure 17, figure 18 and figure 19 show the results obtained for the controlled roll values and the corresponding rate. Figure 17 may be compared to figure 12 to observe the effectiveness of the control design. Similar results were obtained for simulations regarding pitch control.
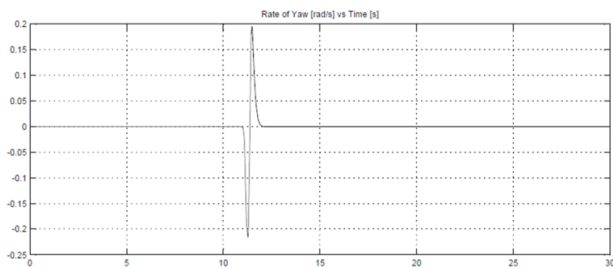

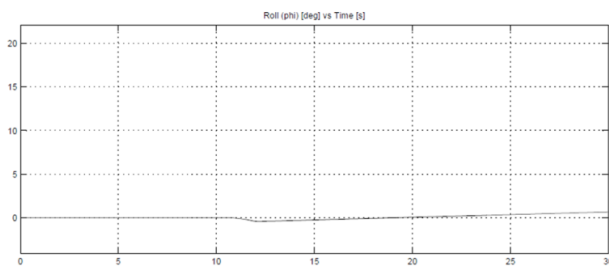**Figure 16.** Graph of Yaw Rate (vertical axis) vs Time (horizontal axis)

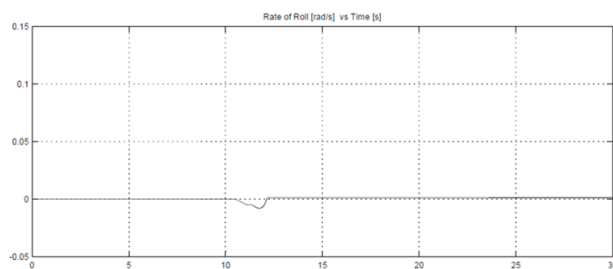**Figure 17.** Graph of Roll (vertical axis) vs Time (horizontal axis)

Figure 18. Graph of angular speed (vertical axis) vs Time (horizontal axis)
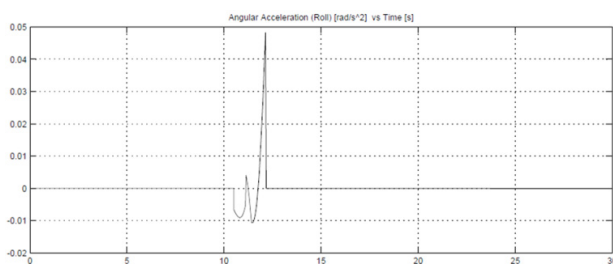

Figure 19. Graph of angular acceleration (vertical axis) vs Time (horizontal axis)

7. Discussion

The linear PD controller design in section 5 of this paper may be sufficient to stabilise the rotorcraft. The only results achieved that were of concern, were those regarding pitch and roll control. It is evident in figure 17, that there is a ramping effect, when the signal should be a constant. This is as a result of integration errors caused due to second-order integration. The original values are computed in the numerical model using equation (53), thus, the angles required are achieved by integration. It is evident in figure 19 that the signal indeed settles, but the mean error carried over in the first integration when computing the rate (figure 18), is translated into a slope when integrated again. This is evident in figure 17. However, these results are acceptable, as they indicate that the controller does effectively stabilise the signal close to the desired reference value. Further, the values that will be fed back to the controller in practice, will not be computed but measured from sensors, thus eliminating these types of errors, but of course, incurring other errors involved with sensors. However, such issues will only be able to be solved once they are encountered.

8. Conclusion

The rotorcraft behaviour described by the simulated model does correlate with what is expected in reality. However, the physical parameters documented are not completely accurate due to the restraining force exerted by the air not being taken into account. In reality, the velocity of the rotorcraft will reach a terminal velocity at some point, and not continue to increase. This phenomenon will be investigated in the near future, as it serves as a subject of importance to the research. However, it extends out of the limits of this paper.

The information obtained from the dynamics model was used for the development of the control system. As shown in section 6.1 of this paper, the rotorcraft will be almost impossible to operate without the implementation of a stabilizing control system. Even the slightest variation of rotor speed can result in a possible crash due to the rotorcraft spinning out of control.

Speed controllers for the electric motors have to be as accurate as possible, with control feedback times kept to a minimum. This will be a challenging task and will require very sensitive gyroscopes, accelerometers and magnetometers to detect when the rotorcraft has strayed off path and requires correction.

To successfully manoeuvre the rotorcraft in the translational x and y directions, the control system must also be used to ensure a torque balance so that the correct heading is obtained. The assistance of a GPS module will

also enhance the directional control of the rotorcraft. The correct angle of attack as well as a preservation of the total upward thrust must also be executed to ensure stability while preserving the direction of the craft.

9. References

1. JC Roos and IK Peddle, "Autonomous Take-off and Landing of an Unmanned Aerial Vehicle", R & D Journal of the South African Institution of Mechanical Engineering, volume 25, pp16-28, 2009
2. D Greer, P McKerrow and J Abrantes, "Robots in Urban Search and Rescue Operations", Australasian Conference on Robotics and Automation, Auckland, pp27-29, 2002
3. V Sikiric, "Control of Quadrocopter", Royal Institute of Technology, Stockholm, Sweden, 2008
4. N Aldawoodi, R Perez, W Alvis and K Valavanis, "Developing Automated Helicopter Models Using Simulated Annealing and Genetic Search", Genetic and Evolutionary Computation Conference, Seattle WA, 2004
5. AA Mian and W Daobo, "Modelling and Backstepping-based Nonlinear Control Strategy for a 6 DOF Quadrotor Helicopter", Chinese Journal of Aeronautics, volume 21, 2008
6. MJ Stepaniak, "A Quadrotor Sensor Platform", Dissertation, Ohio University, Athens, 2008
7. J Kim, MS Kang and S Park, "Accurate Modeling and Robust Hovering Control for a Quad–rotor VTOL Aircraft", Journal of Intelligent Robotic Systems, volume 57, 2010
8. P Pounds, R Mahony and J Gresham, "Towards Dynamically-Favourable Quad-Rotor Aerial Robots", Australasian Conference on Robotics and Automation, Canberra, ACT, 2004
9. JF Douglas, JM Gasiorek, JA Swaffield and LB Jack, "Fluid Mechanics", 5th Edition, Pitman Publishing Limited, 2005
10. S Bouabdallah and R Siegwart, "Full Control of a Quadrotor", International Conference on Intelligent Robots and Systems, 2007
11. A Tewari, "Atmospheric and Space Flight Dynamics: Modeling and Simulation with MATLAB and Simulink", Birkhäuser Boston, 2007
12. P Castillo, R Lozano and AE Dzul, "Modelling and Control of Mini-Flying Machines", Springer-Verlag London Limited, 2005
13. P Castillo, A Dzul and R Lozano, "Real-Time Stabilization and Tracking of a Four Rotor Mini-Rotorcraft", IEEE Transactions on Control Systems Technology, volume 12, 2004
14. S Bouabdallah, "Advances in Unmanned Aerial Vehicles: Design and Control of Miniature Quad rotors", Springer Press, 2007
15. H Huang, GM Hoffmann, SL Waslander and GJ Tomlin, "Aerodynamics and Control of Autonomous Quadrotor Helicopters in Aggressive Maneuvering", IEEE International Conference on Robotics and Automation, Japan, 2009
16. MATLAB® Simulink®, 2010

www.intechweb.org
www.intechopen.com

Yogianandh Naidoo, Riaan Stopforth and Glen Bright: 149
Quad-Rotor Unmanned Aerial Vehicle Helicopter Modelling & Control